Generating Smooth Curves in 3 Dimensions by Minimizing Higher Order Strain Energy Measures

by

Sigrid Adriaenssens, Samar Malek, Masaaki Miki and Chris J K Williams

Reprinted from

INTERNATIONAL JOURNAL OF
SPACE STRUCTURES
Volume 28 · Number 3 & 4 · 2013

MULTI-SCIENCE PUBLISHING CO. LTD.
5 Wates Way, Brentwood, Essex CM15 9TB, United Kingdom

Generating Smooth Curves in 3 Dimensions by Minimizing Higher Order Strain Energy Measures

Sigrid Adriaenssens, Samar Malek, Masaaki Miki and Chris J K Williams*

Princeton University, University of Bath, University of Tokyo, University of Bath

(Submitted on 18/01/2013, Reception of revised paper 28/06/2013, Accepted on 11/09/2013)

ABSTRACT: Elastic beams or rods in two and three dimensions produce smooth curves by minimizing the strain energy due to classical Euler-Bernoulli bending and Saint-Venant torsion subject to constraints on the arc length and end positions and orientations.

However it is possible to postulate other strain energy measures. In this paper we describe a strain energy measure which is the sum of the square of the rate of change of curvature and the square of the product of the curvature and the Frenet torsion.

Key Words: curvature, torsion, elastica, euler spiral, clothoid, cornu spiral, railway transition curve

1. INTRODUCTION

Traditionally smooth curves were constructed on a drawing board using a flexible wooden spline which was pinned to the board at intervals. The spline automatically minimizes the strain energy due to bending and forms sections of elastica between the pinned constraints where there are discontinuities in the rate of change of curvature. The 'best' curve is the one with the fewest pins, allowing the spline itself to define the geometry.

There are many possible strain energy measures, but it could be argued that a 'good' measure only requires one dimensional constant, whose actual value does not influence the final shape. Here we will consider the minimization of the line integral of the sum of the square of the rate of change of curvature and the square of the product of the curvature and the Frenet torsion. The rate of change of curvature and the product of the curvature and torsion both have dimensions 1/length^2.

2. A TRUSS ANALOGY AND PROBLEM STATEMENT

Figure 1 shows a two dimensional pin-jointed truss in its bent and unbent forms. The thick members are inextensible and the thin members are elastic.

The bending from straight is caused entirely by a change in length in the four red members at the ends of the truss. There are no loads or end forces or moments applied to the truss. Thus the truss is a form of mechanism in which modifying only its end curvature causes the entire structure to bend. The end curvature is controlled 'internally' by the red members rather than 'externally' by applying a moment.

Now let us imagine that we apply end forces and moments to the truss. Then close examination of the truss shows that the sagging bending moment between the $(i - 1)^{th}$ and the i^{th} diamond shaped elements is proportional to

*Corresponding author e-mail: c.j.k.williams@bath.ac.uk

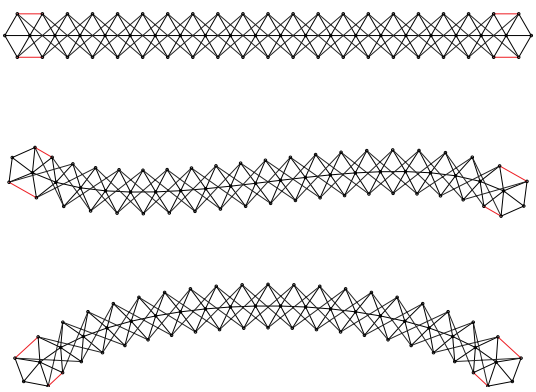

Figure 1. Truss forming Euler spiral.

$$\begin{aligned} &-(\lambda_{i+1}-2\lambda_i+\lambda_{i-1})+(\lambda_i-2\lambda_{i-1}+\lambda_{i-2}) \\ &\quad=-(\lambda_{i+1}-3\lambda_i+3\lambda_{i-1}-\lambda_{i-2}) \end{aligned} \tag{1}$$

where λ_i is the anticlockwise rotation of the i^{th} element and the angle changes between successive elements is assumed to be small. Thus the bending of the truss is controlled by the discrete version of the equation (31) which we shall derive using virtual work.

Because the trusses in the figure are unloaded, the bottom truss is approximately circular and it would be exactly circular but for non-linearity caused by the finite angle change between truss elements. Similarly the middle truss would be exactly an Euler spiral, also known as a Cornu spiral or the clothoid, but for the finite angle change. The Euler spiral is defined as the plane curve whose curvature varies linearly with arc length and it includes the circle as a special case.

In this paper we will consider the 'active bending' of beams or rods with the property of this truss, except that they will produce exactly the Euler spiral when free to move and rotate at their ends. We will also apply end forces and moments which will deform the Euler spiral elastically, enabling a far larger range of curvature/arc length relationships.

The fact that we could make a physical truss with these properties shows that we can use engineering concepts such as bending moment, axial force and shear force in discussion of this type of truss and the equivalent continuous beam-like structure.

3. PREVIOUS WORK

The elastica in two dimensions minimize the strain energy in bending of elastic rods. In the Euler-Bernoulli theory curvature is proportional to bending moment, and therefore the strain energy is proportional to the integral of the square of the curvature. Following [1–4] and [5] we will investigate curves which minimize the integral of the square of the *rate of change of curvature*. The curve will 'want' to form an Euler spiral, but end constraints may prevent this.

Ordinary rods in three dimensions may have strain energy due to both bending and 'twisting'. The 'twisting' is the twist per unit length associated with a material frame, that is a frame which rotates with the material of the rod. The Saint-Venant torsional moment is proportional to the twist per unit length and sections such as 'I' beams also have a Vlasov torsional moment due to warping which is proportional to the second derivative of the twist per unit length.

Harary and Tal [6] minimize the sum of the square of the rate of change of curvature and the square of the rate of change of Frenet torsion. However we will replace the rate of change of Frenet torsion by the product of the curvature and the Frenet torsion.

The Frenet torsion is the twist per unit length of the Frenet frame, one of whose axes is parallel to the curvature vector. The Frenet frame and therefore the Frenet torsion is undefined when the curvature is zero, but in our case that does not matter since the product of the curvature and the Frenet torsion will be zero.

Langer and Singer [7] describe three possible frames, *the Frenet frame*, *a material frame*, and *a natural frame*. A natural frame is one which does not rotate about the tangent to the curve as we move along the curve. We could add a fourth, the superelevation, cant or banking of a railway or road, particularly given the use of Euler spirals as railway transition curves. We shall see that the deformed Euler spiral could also be used as a transition curve with the ability to give continuity to the *rate of change of curvature* as well as just curvature.

Bertails-Descoubes [8] has used the Euler spiral as a finite element shape function for the simulation of curves whose strain energy is proportional to the square of the change in curvature from some pre-bent state. However here we are not primarily concerned with shape functions for approximating curves, but with the properties of the deformed Euler spiral itself.

Our 'twisting' strain energy measure will be associated with the classical Frenet frame [9–10] and therefore we do not need to consider other frames. The two dimensional truss in figure 1 could be made physically, but it should be emphasised that it is doubtful whether a real system could be constructed with our twisting strain energy measure in three

dimensions. This is because real work must be associated with a real frame, namely the material frame. If one were to attempt to construct a real model, one could start by thinking about a very thin, narrow metal ribbon for which the Frenet frame and the material frame coincide and which has the interesting property that it can be bent without twisting, but cannot be twisted without being bent [11]. However the strain energy of a ribbon is given by the Sadowsky functional [12] which is different to that which we propose.

We will now summarise the geometric notation to be used. We can write a curve in the parametric form

$$\mathbf{r}\,(u) = x\,(u)\,\mathbf{i} + y\,(u)\,\mathbf{j} + z\,(u)\,\mathbf{k}$$

in which **i**, **j** and **k** are unit vectors in the directions of the Cartesian x, y and z axes and u is the parameter. The arc length,

$$s = \int \sqrt{\frac{d\mathbf{r}}{du} \cdot \frac{d\mathbf{r}}{du}}\, du$$

and

$$\mathbf{T} = \frac{d\mathbf{r}}{ds} = \frac{\dfrac{d\mathbf{r}}{du}}{\sqrt{\dfrac{d\mathbf{r}}{du} \cdot \dfrac{d\mathbf{r}}{du}}} \tag{2}$$

is the unit tangent. If a rod is inextensible it is natural to use s as the parameter instead of u.

The principal normal is the unit vector **N** and the curvature is the positive scalar κ, both defined by

$$\kappa\mathbf{N} = \frac{d\mathbf{T}}{ds}. \tag{3}$$

The binormal unit vector is perpendicular to both **T** and **N**,

$$\mathbf{B} = \mathbf{T} \times \mathbf{N} \tag{4}$$

and the Frenet torsion is defined by the scalar

$$\tau = \mathbf{B} \cdot \frac{d\mathbf{N}}{ds} = -\frac{d\mathbf{B}}{ds} \cdot \mathbf{N}. \tag{5}$$

The mutually perpendicular unit vectors, **T**, **N** and **B** form the Frenet frame and their rates of change are summarised by the Frenet formulae:

$$\begin{aligned} \frac{d\mathbf{T}}{ds} &= \kappa\mathbf{N} \\ \frac{d\mathbf{N}}{ds} &= -\kappa\mathbf{T} + \tau\mathbf{B} \\ \frac{d\mathbf{B}}{ds} &= \tau\mathbf{N}. \end{aligned} \tag{6}$$

4. KINEMATICS OF RODS AND THE VIRTUAL WORK THEOREM

If we are going to use engineering concepts like bending moment, then we need some way of linking them with geometry and the best way to do this is through virtual work. The virtual work method was developed by Jean Bernoulli, D'Alembert and Lagrange. The French, *principe des puissances virtuelles* (principal of virtual power), is a better description since the virtual displacement has to be infinitesimal and it is therefore better to use a virtual velocity and the corresponding virtual power.

Let us imagine a rod that is moving with time t so that the position of a typical point on the rod is $\mathbf{r}\,(u, t)$. We have used u rather than the arc length s since the rod might stretch, although later we will impose the condition of inextensiblity.

The velocity of a point on the rod is

$$\mathbf{V} = \frac{\partial \mathbf{r}}{\partial t} \tag{7}$$

and for our purposes we can think of this as being a real (as opposed to virtual) velocity of a rod that is moving to minimize its elastic strain energy.

The rate of change of velocity with position along the rod is

$$\frac{\partial \mathbf{V}}{\partial u} = \left|\frac{\partial \mathbf{r}}{\partial u}\right| (\boldsymbol{\Omega} \times \mathbf{T} + \epsilon\mathbf{T}) \tag{8}$$

in which $\boldsymbol{\Omega}$ is the angular velocity of the rod and $\in$ is the rate of axial strain. The component of angular velocity tangential to the curve, $\boldsymbol{\Omega} \cdot \mathbf{T}$, makes no contribution to the rate of change of velocity and would be associated with the frame transmitting the torsional moment. This would normally be the material frame but in our case it is a combination of the Frenet frame and a natural frame so that we have two values of $\boldsymbol{\Omega} \cdot \mathbf{T}$. This will be explained later.

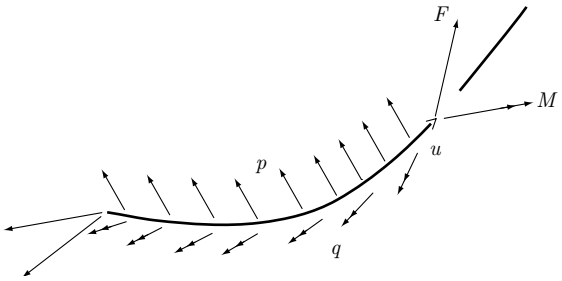

Figure 2. Force and moment crossing a cut.

(8) is the compatibility equation which will enable us to find the equilibrium relationship between the loads applied to the rod and the internal forces and moments within the rod and also to find an expression for the work being done on the rod.

The rod is loaded with a force $\mathbf{p}$ and couple $\mathbf{q}$ per unit arc length and $\mathbf{F}$ and $\mathbf{M}$ are the force and moment crossing the imaginary cut in the rod shown in figure 2. We will assume that the rod is moving slowly so that there are no inertia effects.

The total rate of work being done by the loads and end forces is

$$W = [\mathbf{\Omega}\cdot\mathbf{M} + \mathbf{V}\cdot\mathbf{F}]_{u_0}^{u_1} + \int_{u_0}^{u_1} (\mathbf{\Omega}\cdot\mathbf{q} + \mathbf{V}\cdot\mathbf{p})\left|\frac{\partial\mathbf{r}}{\partial u}\right| du \quad (9)$$

in which u_0 and u_1 are the values of u at the ends of the rod.

We can rewrite W as

$$\begin{aligned} W = \int_{u_0}^{u_1} \Bigg(& \frac{\partial\mathbf{\Omega}}{\partial u}\cdot\mathbf{M} + \mathbf{\Omega}\cdot\frac{\partial\mathbf{M}}{\partial u} + \frac{\partial\mathbf{V}}{\partial u}\cdot\mathbf{F} \\ & + \mathbf{V}\cdot\frac{\partial\mathbf{F}}{\partial u} + (\mathbf{\Omega}\cdot\mathbf{q} + \mathbf{V}\cdot\mathbf{p})\left|\frac{\partial\mathbf{r}}{\partial u}\right| \Bigg) du \end{aligned} \quad (10)$$

and therefore using (8) and the scalar triple product,

$$W = \int_{u_0}^{u_1} \begin{pmatrix} \dfrac{\partial\mathbf{\Omega}}{\partial u}\cdot\mathbf{M} + \epsilon\mathbf{T}\cdot\mathbf{F}\left|\dfrac{\partial\mathbf{r}}{\partial u}\right| \\ +\mathbf{\Omega}\cdot\left(\dfrac{\partial\mathbf{M}}{\partial u} + (\mathbf{T}\times\mathbf{F} + \mathbf{q})\left|\dfrac{\partial\mathbf{r}}{\partial u}\right|\right) \\ +\mathbf{V}\cdot\left(\dfrac{\partial\mathbf{F}}{\partial u} + \mathbf{p}\left|\dfrac{\partial\mathbf{r}}{\partial u}\right|\right) \end{pmatrix} du. \quad (11)$$

This applies for any real or virtual $\mathbf{\Omega}$ and $\mathbf{V}$ and also for any limits u_0 and u_1 and therefore

$$\frac{d\mathbf{M}}{ds} + \mathbf{T}\times\mathbf{F} + \mathbf{q} = 0 \quad (12)$$

and

$$\frac{d\mathbf{F}}{ds} + \mathbf{p} = 0 \quad (13)$$

which are the equations of static equilibrium of moments and forces. We have replaced the parameter u by arc length and the partial derivatives by ordinary derivatives since the velocity and angular velocity do not appear and all quantities can be considered to be independent of time. (12) can be rearranged to give

$$\mathbf{F} = \mathbf{T}\times\left(\frac{d\mathbf{M}}{ds} + \mathbf{q}\right) + F_{\text{tension}}\mathbf{T} \quad (14)$$

where F_{tension} is the tension in the rod.

Thus, returning to (9) and (11), we have

$$\begin{aligned} & [\mathbf{\Omega}\cdot\mathbf{M} + \mathbf{V}\cdot\mathbf{F}]_{u_0}^{u_1} + \int_{u_0}^{u_1} (\mathbf{\Omega}\cdot\mathbf{q} + \mathbf{V}\cdot\mathbf{p})\left|\frac{\partial\mathbf{r}}{\partial u}\right| \partial u \\ & = \int_{u_0}^{u_1} \left(\frac{\partial\mathbf{\Omega}}{\partial u}\cdot\mathbf{M} + \epsilon\mathbf{T}\cdot\mathbf{F}\right)\left|\frac{\partial\mathbf{r}}{\partial u}\right| du \end{aligned} \quad (15)$$

which is the virtual work equation. The left hand side is the rate of virtual work being done by the end forces and moments and the forces and couples applied along the length of the rod. The right hand side is the rate of work being absorbed by bending, twisting and stretching the rod. It is important to note that this equation applies to all rods, elastic or non-elastic, initially straight or initially curved. It also applies in a modified form to rods with extra degrees of flexibility such as the shear flexibility of a Cosserat rod or Timoshenko beam, in which case extra terms have to be added to both sides of the equation.

If the rod is inextensible we lose the ϵ term and we can also use the arc length as the parameter to give

$$\begin{aligned} & [\mathbf{\Omega}\cdot\mathbf{M} + \mathbf{V}\cdot\mathbf{F}]_{s_0}^{s_1} + \int_{s_0}^{s_1} (\mathbf{\Omega}\cdot\mathbf{q} + \mathbf{V}\cdot\mathbf{p}) ds \\ & = \int_{s_0}^{s_1} \frac{\partial\mathbf{\Omega}}{\partial s}\cdot\mathbf{M} ds. \end{aligned} \quad (16)$$

We will equate the right hand side of this equation to the rate of change of strain energy due to bending and twisting the Euler spiral and for our purposes the most important aspect of (16) is that it enables us to say that the bending and twisting moment $\mathbf{M}$ is that part of the right hand side of the virtual (or real) work equation scalar multiplied by $\dfrac{\partial \boldsymbol{\Omega}}{\partial s}$.

5. THE DEFORMED EULER SPIRAL

We will now introduce the strain energy measure for the deformed Euler spiral. Differentiating the first Frenet formula,

$$\frac{d^2\mathbf{T}}{ds^2} = -\kappa^2\mathbf{T} + \frac{d\kappa}{ds}\mathbf{N} + \kappa\tau\mathbf{B} \tag{17}$$

whose component perpendicular to $\mathbf{T}$ is

$$\begin{aligned}\mathbf{X} &= \frac{d^2\mathbf{T}}{ds^2} - \left(\frac{d^2\mathbf{T}}{ds^2}\cdot\mathbf{T}\right)\mathbf{T} = \frac{d^2\mathbf{T}}{ds^2} \\ &+ \left(\frac{d\mathbf{T}}{ds}\cdot\frac{d\mathbf{T}}{ds}\right)\mathbf{T} = \frac{d\kappa}{ds}\mathbf{N} + \kappa\tau\mathbf{B}.\end{aligned} \tag{18}$$

The scalar product

$$\mathbf{X}\cdot\mathbf{X} = \frac{d^2\mathbf{T}}{ds^2}\cdot\frac{d^2\mathbf{T}}{ds^2} - \left(\frac{d\mathbf{T}}{ds}\cdot\frac{d\mathbf{T}}{ds}\right)^2 = \left(\frac{d\kappa}{ds}\right)^2 + \kappa^2\tau^2 \tag{19}$$

and we will define the strain energy as

$$U = \frac{\beta}{2}\int_{s_0}^{s_1}\mathbf{X}\cdot\mathbf{X}ds = \frac{1}{2}\beta\int_{s_0}^{s_1}\left(\left(\frac{d\kappa}{ds}\right)^2 + \kappa^2\tau^2\right)ds \tag{20}$$

in which β is a constant corresponding to the *EI* of the elastica. Note that we could alternatively have used $U = \beta/2\int_{s_0}^{s_1} d^2\mathbf{T}/ds^2\cdot d^2\mathbf{T}/ds^2 ds$ but this would not have included the Euler spiral as a special case.

Harary and Tal [6] use the Euler-Lagrange equation to minimize the strain energy, but we shall proceed from first principals since it is then easier to isolate the bending and twisting moments. We will again assume that our rod is moving, but impose the requirement of inextensibility so that we can continue to use the arc length as a parameter. Then (8) becomes

$$\frac{\partial\mathbf{T}}{\partial t} = \frac{\partial^2\mathbf{r}}{\partial s\partial t} = \frac{\partial\mathbf{V}}{\partial s} = \boldsymbol{\Omega}\times\mathbf{T} \tag{21}$$

and hence after some manipulation,

$$\begin{aligned}&\frac{1}{2}\frac{\partial}{\partial t}(\mathbf{X}\cdot\mathbf{X}) = \\ &\frac{\partial^2\boldsymbol{\Omega}}{\partial s^2}\cdot\left(\mathbf{T}\times\frac{\partial^2\mathbf{T}}{\partial s^2}\right) + 2\frac{\partial\boldsymbol{\Omega}}{\partial s}\cdot \\ &\left[\frac{\partial\mathbf{T}}{\partial s}\times\left(\frac{\partial^2\mathbf{T}}{\partial s^2} - \left(\frac{\partial^2\mathbf{T}}{\partial s^2}\cdot\mathbf{T}\right)\mathbf{T}\right)\right].\end{aligned} \tag{22}$$

After some further manipulation

$$\frac{\beta}{2}\frac{\partial}{\partial t}(\mathbf{X}\cdot\mathbf{X}) = \beta\frac{\partial}{\partial s}\left[\frac{\partial\boldsymbol{\Omega}}{\partial s}\cdot\left(\mathbf{T}\times\frac{\partial^2\mathbf{T}}{\partial s^2}\right)\right] + \frac{\partial\boldsymbol{\Omega}}{\partial s}\cdot\mathbf{M} \tag{23}$$

where the moment in the rod is

$$\begin{aligned}\mathbf{M} = \beta\Bigg[&2\frac{\partial\mathbf{T}}{\partial s}\times\left(\frac{\partial^2\mathbf{T}}{\partial s^2} - \left(\frac{\partial^2\mathbf{T}}{\partial s^2}\cdot\mathbf{T}\right)\mathbf{T}\right) \\ &- \frac{\partial}{\partial s}\left(\mathbf{T}\times\frac{\partial^2\mathbf{T}}{\partial s^2}\right)\Bigg] + \mu\mathbf{T}\end{aligned} \tag{24}$$

which is that part of (23) scalar multiplied by $\dfrac{\partial\boldsymbol{\Omega}}{\partial s}$.

Note that upon integration we will have an extra term

$$\beta\frac{\partial\boldsymbol{\Omega}}{\partial s}\cdot\left(\mathbf{T}\times\frac{\partial^2\mathbf{T}}{\partial s^2}\right) \tag{25}$$

at each end of the rod which corresponds to the fact that we will be able to specify the curvature at the rod ends as well as position and orientation and this may be associated with 'doing some work'.

We can now return to the static case so that we can drop the partial derivatives in (24),

$$\begin{aligned}\mathbf{M} = \beta\Bigg[&2\frac{d\mathbf{T}}{ds}\times\left(\frac{\partial^2\mathbf{T}}{\partial s^2} - \left(\frac{\partial^2\mathbf{T}}{\partial s^2}\cdot\mathbf{T}\right)\mathbf{T}\right) \\ &- \frac{d}{ds}\left(\mathbf{T}\times\frac{d^2\mathbf{T}}{ds^2}\right)\Bigg] + \mu\mathbf{T}\end{aligned} \tag{26}$$

and then using (17) and the Frenet formulae (6),

$$\begin{aligned}\mathbf{M} = \beta\Bigg[&\kappa^2\tau\mathbf{T} + \left(2\frac{d\kappa}{ds}\tau + \kappa\frac{d\tau}{ds}\right) \\ &\mathbf{N} - \left(\frac{d^2\kappa}{ds^2} - \kappa\tau^2\right)\mathbf{B}\Bigg] + \mu\mathbf{T}.\end{aligned} \tag{27}$$

μ is *constant along the curve* and $\mu\mathbf{T}$ is a torsional moment or torque in addition to the $\beta\kappa^2\tau\mathbf{T}$ which is associated with the Frenet frame. $\mu\mathbf{T}$ is associated with a natural frame, or possibly a material frame if we prefer to include some St. Venant torsional flexibility.

If the rod were rotating about its axis, power could be transferred by the $\mu\mathbf{T}$ from one end to the other, exactly as in a flexible drill shaft. This constant torque is analogous to the tension in (14) in that both can only by determined by end constraints or applied force or moment.

If there is no couple $\mathbf{q}$ applied along the length of the rod, then (13) and (14) tell us that an applied load

$$\mathbf{p}_\mu = -\frac{d}{ds}\left(\mu\mathbf{T}\times\frac{d\mathbf{T}}{ds}\right) = -\mu\mathbf{T}\times\frac{d^2\mathbf{T}}{ds^2} \qquad (28)$$

will balance the effect of the constant torque. This is useful in that it means that a constant torque can be replaced by minus this load. It also tells us that a flexible drill shaft is in equilibrium provided that the shaft is bent in a circle.

6. THE DEFORMED EULER SPIRAL IN TWO DIMENSIONS

In two dimensions the moment equation can be written

$$M = M_0 + F_x\dot{y}. \qquad (29)$$

Moment is a scalar in two dimensions and M_0 and F_x are both constant. We have rotated our axes so that the y component of force, F_y is zero. In fact we only need one constant because M_0 can be included in a change of origin for y, but we need M_0 for the case when $F_x = 0$.

Therefore we have

$$\beta\frac{d^2\kappa}{ds^2} + M_0 + F_x y = 0. \qquad (30)$$

Thus if the force and M_0 are both zero, the rate of change of curvature $d\kappa/ds$ is constant which is the equation of the Euler spiral, including the circle as a special case. Any applied moment will then bend the Euler spiral.

Note that a point load causes a discontinuity in $d^2\kappa/ds^2$ whereas a point load on a conventional elastic spline causes a discontiuity in $d\kappa/ds$.

If we use intrinsic coordinates, $dx/ds = \cos\lambda$ and $dy/ds = \sin\lambda$,

$$\beta\frac{d^3\lambda}{ds^3} + M_0 + F_x y = 0. \qquad (31)$$

This equation was integrated numerically to produce Figures 3 to 6. For given M_0 and F_x it is possible to march along the curve from starting values of y, λ, $d\lambda/ds$ and $d^2\lambda/ds^2$.

Figure 3 shows the effect of applying a constant moment to the Euler spiral for which equation (30) tells us that the curvature is a parabolic function of arc length. The different curves have different values of moment, but they all start at the top of the circle with the same curvature, going to the left or the right. All the curves have the same total length, the ones that look shorter are partly hidden by the circle before they peel away. Dillen [13] discusses curves whose curvatures are polynomial functions of arc length.

Figure 4 shows the deformed Euler spiral with different values of applied force, all along the same line of action, shown by the horizontal line. Again they all start at the top of the circle with the same curvature.

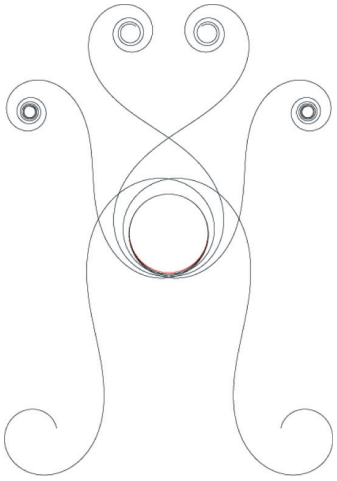

Figure 3. Deformed Euler spirals with different values of constant applied moment.

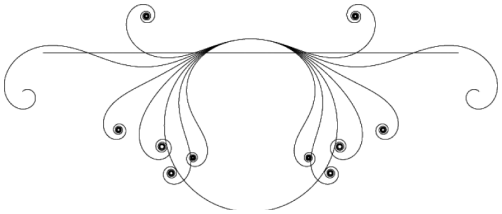

Figure 4. Deformed Euler spirals of the same length, with different values of applied force, all along the same line of action, shown by the horizontal line.

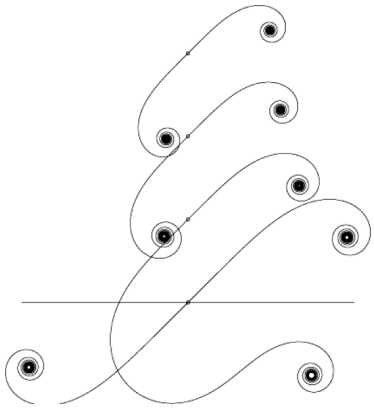

Figure 5. Deformed Euler spirals with the same applied compressive force, all along the same line of action, shown by the horizontal line.

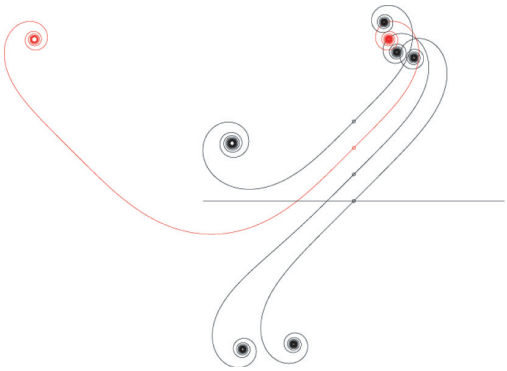

Figure 6. Deformed Euler spirals with the same applied tensile force, all along the same line of action, shown by the horizontal line.

Figures 5 and 6 show deformed Euler spirals with the same applied force, compressive in Figure 5 and tensile in Figure 6, all along the same line of action. The curves all start from the small circle near their middles, in opposite directions, from an initial point at which there is *zero curvature and zero rate of change of curvature*.

The red curve in Figure 6 is symmetric about a line parallel to the y axis and it therefore contains two points with zero curvature and rate of change of curvature, making it a good railway transition curve, which we will discuss further in the next section.

7. THE DEFORMED EULER SPIRAL IN THREE DIMENSIONS AND THE FINITE ELEMENT METHOD

The technique of marching along a curve that was applied in two dimensions can also be applied in three dimensions. However the problem of finding initial conditions which will produce a symmetric curve or cause a curve to pass through a known end point has to be solved. The symmetric red curve in Figure 6 was produced by trial and error. Ideally we want to specify the same number of boundary conditions at both ends, rather than all at one end.

Figure 7 was produced using the finite element method using a four noded element based on a cubic B-spline. Many different end conditions could be applied and in this case the ends are fixed in position, the curvature is zero and a bending moment is applied such that the rate of change of curvature is zero. An additional constant torsional moment is modelled using (28) which makes the curve three dimensional, antisymmetric in elevation, but symmetric in plan.

The black curve in figure 8 shows the curvature of the curve in figure 7 as a function of arc length. The curvature is almost indistinguishable from the quartic $k_{\max}\ (1-s)^2(1+s)^2$ in which $k_{\max}$ is the maximum curvature and s is scaled so that $s = \pm 1$ at the two ends of the curve.

As discussed above, we could minimize $d^2\mathbf{T}/ds^2 \cdot d^2\mathbf{T}/ds^2$ instead of $\mathbf{X} \cdot \mathbf{X}$ which would introduce an extra term $2\beta\kappa^3\mathbf{B}$ in the expression for moment, (27). This slightly reduces the maximum curvature as shown by the red line in figure 8 and extends the curvature over slightly longer distance. However it would make more difference to the coils at the end of a spiral where the curvature is large.

The conventional Euler spiral transition curve - circle - transition curve consists of a section with linearly increasing curvature followed by a constant curvature section followed by a linear curvature

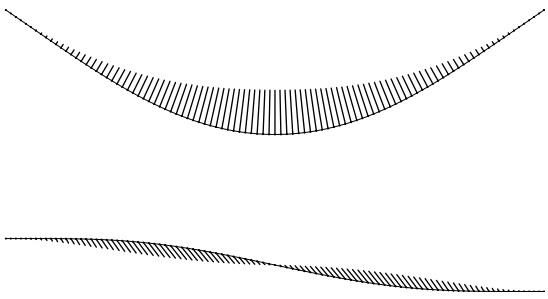

Figure 7. Deformed Euler spiral in three dimensions, showing curvature vectors, plan top and elevation bottom.

Figure 8. Curvature as a function of arc length for the the minimization $\mathbf{X} \cdot \mathbf{X}$ in black and of $d^2\mathbf{T}/ds^2 \cdot d^2\mathbf{T}/ds^2$ in red.

decrease. The cant or superelevation of a railway track should be proportional to the curvature. Therefore the rate of change of superelevation, that is the angular velocity about the train axis, is proportional to rate of change of curvature. Thus entering or leaving a conventional Euler spiral should theoretically be accompanied by an unpleasant discontinuity in angular velocity about the train axis. It is also worth noting that a transition curve should apply to the path of the passengers, not to the rails, some distance below. In order to turn to the right a small deviation of the track to the left is first required, exactly as in the path of a bicycle tyre on the road [14].

8. FUTURE WORK

The deformation of an elastic Euler spriral allows a larger number of end conditions than either the Euler spiral or the elastica and we have only considered one set.

The curves in this paper have been found numerically, and this does not preclude some analytic solutions, but the need for elliptic integrals for the elastica and Fresnel integrals for the Euler spiral suggests that this may be difficult. However, a Euler spiral can be bent into helix in very much the same way as a conventional Euler-Bernoulli rod by a combination of a moment about the axis of the helix and a constant torque about the tangent to the curve.

We can also consider higher derivatives. If we write

$$\mathbf{X}_n = \frac{d\mathbf{X}_{n-1}}{ds} - \left(\frac{d\mathbf{X}_{n-1}}{ds} \cdot \mathbf{T} \right) \mathbf{T} \tag{32}$$

where

$$\mathbf{X}_0 = \frac{d\mathbf{T}}{ds} = \kappa \mathbf{N} \tag{33}$$

(so that $\mathbf{X}$ in (18) is $\mathbf{X}_1$) we could minimize the integral $\beta/2 \int \mathbf{X}_n \cdot \mathbf{X}_n ds$. In two dimensions this would result in a bending moment

$$M = (-1)^n \beta \frac{d^{2n}\kappa}{ds^{2n}} \tag{34}$$

which includes Euler-Bernoulli bending as a special case when $n = 0$ and $\beta = EI$.

The $(-1)^n$ in (34) can be understood by looking at the truss in figure 1 in which the tops and bottoms of next but one diamonds are laced with elastic members. This corresponds to $n = 1$ in (34). To produce a truss with the properties of an Euler-Bernoulli beam we would have to join the tops of successive diamonds with elastic members and also the bottoms of successive diamonds.

Thus if we are to produce trusses which model different values of n by using different lacing patterns we can expect top to bottom lacing to produce odd n values and top to top and bottom to bottom to produce even values. Higher derivatives are modelled by connecting more distant diamonds with elastic members.

REFERENCES

[1] Even Mehlum. *Curve and surface fitting based on variational criteriae for smoothness*. PhD thesis, University of Oslo, Norway, 1969.

[2] Henry Packard Moreton. *Minimum Curvature Variation Curves, Networks, and Surfaces for Fair Free-Form Shape Design*. PhD thesis, University of California at Berkeley, 1992.

[3] Benjamin B. Kimia, Ilana Frankel, and Ana-Maria Popescu. Euler spiral for shape completion. *International Journal of Computer Vision*, 54:159–182, 2003.

[4] D.J. Walton and D.S. Meek. An improved Euler spiral algorithm for shape completion. In *Canadian Conference on Computer and Robot Vision, 2008*. CRV 08, pages 237–244, May 2008.

[5] Hailing Zhou, Jianmin Zheng, and Xunnian Yang. Euler arc splines for curve completion. *Computers & Graphics*, 36(6):642–650, 2012.

[6] Gur Harary and Ayellet Tal. 3D Euler spirals for 3D curve completion. *Computational Geometry*, 45(3):115–126, 2012.

[7] Joel Langer and David Singer. Lagrangian aspects of the kirchhoff elastic rod. *SIAM Review*, 38(4):pp. 605–618, 1996.

[8] Florence Bertails-Descoubes. Super-clothoids. *Computer Graphics Forum*, 31(2pt2):509–518, 2012.

[9] Dirk J. Struik. *Lectures on Classical differential Geometry*. Addison-Wesley, 1961.

[10] Luther Pfahler Eisenhart. *An introduction to differential geometry, with use of the tensor calculus*. Princeton University Press, 1947.

[11] L. Giomi and L. Mahadevan. Statistical mechanics of developable ribbons. *Phys. Rev. Lett.*, 104:238104, June 2010.

[12] T. Hangan. Elastic strips and differential geometry. *Rendiconti del Seminario Matematico*, 63:179–186, 2005.

[13] F. Dillen. The classification of hypersurfaces of a euclidean space with parallel higher order fundamental form. *Mathematische Zeitschrift*, 203:635–643, 1990.

[14] J. Fajans. Steering in bicycles and motorcycles. *American Journal of Physics*, 68(7):654–659, 2000.